Mon. Not. R. Astron. Soc. **000**, 1–10 () Printed 18 September 2006 (MN LaTeX style file v2.2)

Optical spectroscopy of high proper motion stars: new M dwarfs within 10 pc and the closest pair of subdwarfs

C. Reylé[1⋆], R.-D. Scholz[2], M. Schultheis[1], A. C. Robin[1] and M. Irwin[3]
[1] *CNRS UMR6091, Observatoire de Besançon, BP 1615, 25010 Besançon Cedex, France*
[2] *Astrophysikalisches Institut Potsdam, An der Sternwarte 16, Potsdam, D-14482, Germany*
[3] *Institute of Astronomy, University of Cambridge, Madingley Road, Cambridge, CB3 0HA, England*

Accepted . Received ; in original form

ABSTRACT
We present spectra of 59 nearby stars candidates, M dwarfs and white dwarfs, previously identified using high proper motion catalogues and the DENIS database. We review the existing spectral classification schemes and spectroscopic parallax calibrations in the near-infrared J-band and derive spectral types and distances of the nearby candidates. 42 stars have spectroscopic distances smaller than 25 pc, three of them being white dwarfs. Two targets lie within 10 pc, one M8 star at 10.0 pc (APMPM J0103-3738), and one M4 star at 8.3 pc (LP 225-57). One star, LHS 73, is found to be among the few subdwarfs lying within 20 pc. Furthermore, together with LHS 72, it probably belongs to the closest pair of subdwarfs we know.

Key words: Galaxy: solar neighbourhood – stars: late type – white dwarfs – subdwarfs

1 INTRODUCTION

Recent discoveries of cool objects, such as M stars or brown dwarfs, closer than 5 parsecs show that even the immediate solar neighbourhood sample is still incomplete (Delfosse et al. 2001; Scholz et al. 2003; Teegarden et al. 2003; Hambly et al. 2004).

Henry et al. (1997) estimated that about 130 systems over 359 (36%) are missing within 10 pc. The missing fraction is even larger within 25 pc (63%) with a deficit of about 3500 systems over the 5500 expected ones (Henry et al. 2002). Statistical comparisons from the local sample in the northern hemisphere led to a less pessimistic result, the current 10 pc sample being ∼75% complete (Reid et al. 2003a).

New surveys in the near infrared such as DENIS (Epchtein et al. 1997) and 2MASS (Cutri et al. 2003) provide unprecedented data for a systematic search for low luminosity cool dwarfs. The use of these data together with high proper motion catalogues is a powerful tool for discovering our neighbours. Hundreds of stars closer than 25 parsecs have been discovered this way (e.g. Phan-Bao et al. 2001, 2003; Reid & Cruz 2002; Reid et al. 2002; Reylé et al. 2002; Reid et al. 2003b, 2004; Hambly et al. 2004; Reylé & Robin 2004; Lodieu et al. 2005; Scholz et al. 2005).

As spectroscopy provides much more information than photometry alone, spectroscopic observations were also carried out to identify and classify nearby stars. Recent studies dealing with sample sizes larger than 10 objects are cited in Table 1. All together, they revealed 490 stars in the 25 pc sample and 25 within 10 pc. However, we note that the samples investigated by the different authors do have many stars in common so that the total number of newly discovered neighbours is much smaller.

Table 1. Nearby stars identified by spectroscopy

Reference	Sample size	Number of stars within 25 pc	10 pc
Cruz & Reid (2002)	70	28	
Henry et al. (2002)	34	6	2
Reid et al. (2003b)	357	127	9
Lodieu et al. (2005)	71	25	3
Crifo et al. (2005)	39	31	1
Scholz et al. (2005)	322	226	8
Phan-Bao & Bessel (2006)	45	5	
This study	59	42	2

In previous papers (Reylé et al. 2002; Reylé & Robin 2004), we have determined the photometric distances of high proper motion stars that we cross-identified with the DENIS survey. We have reported the discovery of 115 nearby candidates, probably lying within 25 pc, the limit of the Catalogue of Nearby Stars (Gliese & Jahreiss 1991, CNS3). We selected the closest candidates for a spectroscopic follow-up performed at La Silla Observatory (Chile).

Our sample of nearby candidates is described in § 2.

⋆ E-mail: celine@obs-besancon.fr

§ 3 describes the spectroscopic observations. In § 4 we review the spectroscopic classification schemes and compute the spectral type of the stars. Computation of distances is detailed in § 5. In § 6 we discuss the chromospheric activity of the stars in our sample and the conclusions are given in § 7.

2 NEARBY CANDIDATES SAMPLE

Due to their small distance, most of the nearby stars have high proper motions. However, many stars in high proper motion catalogues have no distance determined yet. Note that a high proper motion does not imply a short distance but may also indicate a high space velocity with respect to the Sun.

As a contribution towards in improving the completeness of the solar neighbourhood census, we made a systematic search for nearby stars among two new high proper motion catalogues. The cross-identification of those with the DENIS database allowed us to determine the distances of the stars from NIR photometry, an appropriate wavelength range for M-type dwarfs.

In Reylé et al. (2002), we present preliminary distance estimates for 301 APM high proper motion stars (Scholz et al. 2000). 15 stars were found to be within the 25 pc limit of the *Catalogue of Nearby Stars* (CNS3, Gliese & Jahreiss 1991). In Reylé & Robin (2004), we used the Liverpool-Edinburgh high proper motion survey (Pokorny et al. 2003) and found 100 stars that probably lie within 25 parsecs from the Sun. They are mainly M dwarf candidates, with the exception of few white dwarf candidates.

Given the large uncertainties on the photometric distances (up to 45% in some cases), follow-up observations of these candidates were needed. We selected 54 stars, with photometric distances smaller than 20 pc, for spectroscopic follow-up. Using the reduced proper motion versus colour diagram, we showed that these objects are likely M dwarfs, except 5 white dwarf candidates. We also observed 4 stars that could be either disc or thick disc M dwarfs, for which we determined two photometric distances with two metallicity hypotheses. They are nearby candidates if they belong to the thick disc. Finally, we obtained spectra for one star that may be a nearby subdwarf and one star detected in the J and K bands, but not in the I band. Optical and near-IR DENIS photometry, proper motion, as well as photometric distance determination are given in Tables 2 and 3 for the APM and LEHPMS nearby candidates, respectively. Figure 1 shows their reduced proper motion versus colour diagram, where the reduced proper motion is $H = I + 5\log\mu + 5$.

3 SPECTROSCOPIC OBSERVATIONS

In order to insure the spectral types and therefore distances, we carried out spectroscopic observations on the 3.6m New Technology Telescope (NTT) at La Silla Observatory (ESO, Chile) in November 2003. Optical low-resolution spectra were obtained in the Red Imaging and Low-dispersion spectroscopy (RILD) observing mode with the EMMI instrument. The spectral dispersion of the grism we used is 0.28 nm/pix, with a wavelength range 385-950 nm. Except for the white dwarf candidates, we used an order blocking filter to avoid the second order overlap that occurs beyond 800 nm. Thus the effective wavelength coverage ranges from 520 to 950 nm. The slit was 1 arcsec wide and the resulting resolution was 10.4 Å . The seeing varied from 0.5 to 1.5 arcsec. Exposure time ranged from 15 s for the brightest to 120 s for the faintest dwarf ($I = 15.3$). The reduction of the spectra was done using the context *long* of MIDAS. Fluxes were calibrated with the spectrophotometric standards LTT 2415 and Feige 110.

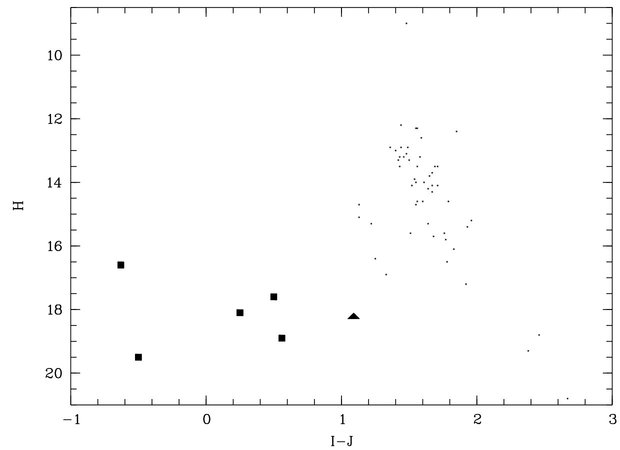

Figure 1. (H,$I - J$) diagram for the high proper motion stars cross-identified with DENIS. Dots: M-dwarfs. Squares: white dwarf candidates. Triangle: subdwarf candidate.

We obtained spectra for 59 nearby candidates. They are shown in Figure 2 and 3. In addition, we observed two radial velocity standard M-stars (Nidever et al. 2002) with spectral type sdM0 and M1, 12 comparison stars with known spectral types from M0 to M6, found in the NASA NStars[1], the ARICNS[2] and the SIMBAD[3] databases, and one M9 star (Delfosse et al. 2001). Discrepancies are found in the spectral types given by the different databases (see Table 4), probably due to the fact that different spectral classification systems are used. These templates, and our finally adopted types are in currently accepted system of Kirkpatrick et al. (1991). Deviations between our adopted sequence and other published spectral types are usually 0.5 to 1 subtype and discrepancies mostly occur at earlier types (M0-M3).

4 SPECTRAL CLASSIFICATION

4.1 M dwarfs

In the past years, several classification schemes have been proposed for cool dwarfs. First, the least-squares minimization technique by Kirkpatrick et al. (1991) has the advantage of assigning types based on both molecular or atomic features and the slope of the spectrum. Recently, Henry et al. (2002) developed a similar but more accurate method that matches a target spectrum to one from a

[1] http://nstars.arc.nasa.gov
[2] http://www.ari.uni-heidelberg.de/aricns/
[3] http://cdsweb.u-strasbg.fr/Simbad

Table 2. Nearby APM star candidates observed at ESO/NTT. B_J and R are from the APM high proper motion catalogue, obtained on digitized plates. I and $I-J$ are from DENIS.

name	α_{J2000}	δ_{J2000}	ESO epoch	μ_x (”yr^{-1})	μ_y	B_J	R	I DENIS	$I-J$	$d_{\rm phot}$ (pc)
LP 291-115	00 33 13.26	-47 33 17.8	1993.7	0.26	0.15	16.45	14.20	12.26	1.79	15.7
APMPM J0103-3738	01 02 49.77	-37 37 46.8	1990.7	1.44	0.30	19.73	17.30	13.83	2.67	12.2
APMPM J0145-3205	01 45 11.27	-32 05 09.6	1991.9	0.58	0.18	13.83	12.14	11.36	1.52	18.4
LP 940-20	01 49 42.37	-33 19 21.5	1991.9	0.38	0.11	16.60	14.36	12.65	1.76	19.6
LHS 5045	01 52 52.07	-48 05 39.2	1988.9	-0.55	-0.20	14.52	12.40	10.77	1.60	11.0
LP 225-57	02 34 20.95	-53 05 35.4	1994.0	0.25	-0.34	12.88	10.78	9.79	1.49	9.6
L 127-33	02 40 36.99	-60 44 48.5	1991.9	0.19	0.29	15.35	13.85	12.34	1.13	116.7/30.4[a]
APMPM J0255-5140	02 55 13.92	-51 40 23.1	1992.8	0.59	0.23	15.03	12.68	11.56	1.67	13.7
LP 831-45	03 14 17.96	-23 09 31.2	1993.0	0.35	0.19	13.29	11.46	9.90	1.44	11.7
LHS 5090	04 04 31.58	-62 59 10.4	1990.0	0.25	-0.46	16.34	14.49	12.85	1.25	103.6/25.5[a]
LHS 1656	04 18 50.80	-57 14 06.0	1995.0	0.27	0.75	12.97	11.02	10.75	1.22	42.5/10.7[a]
APMPM J0541-5349	05 41 27.18	-53 49 17.9	1991.1	0.10	0.37	13.61	11.82	11.77	1.13	90.3/23.6[a]
LP 904-51	10 41 43.77	-31 11 52.7	1993.1	0.37	-0.25	16.80	15.10	12.84	1.83	19.3
APMPM J1107-2202	11 06 45.50	-22 02 16.2	1992.2	0.34	-0.27	13.92	11.87	11.48	1.56	16.8
APMPM J1932-4834	19 31 53.09	-48 33 50.5	1991.6	0.01	-0.37	16.21	14.15	12.39	1.85	15.4
APMPM J2101-4115	21 01 03.44	-41 14 31.8	1991.7	0.36	-0.25	15.40	13.46	11.50	1.55	17.5
APMPM J2101-4907	21 01 07.50	-49 07 23.7	1992.6	-0.31	-0.15	12.01	11.25	10.52	1.43	16.5
LTT 8708 A/B	21 49 11.00	-41 33 28.6	1990.7	0.30	-0.17	12.65	10.06	9.29	1.48	7.8
LHS 3800	22 23 08.90	-43 27 35.3	1990.8	0.79	-0.37	15.39	13.85	12.23	1.33	15.7
LHS 3842	22 40 57.59	-45 43 23.1	1992.6	0.33	-0.30	14.39	12.35	11.30	1.55	16.0
APMPM J2330-4737	23 30 16.48	-47 36 38.2	1992.9	-0.59	-0.95	19.13	17.19	13.70	2.38	15.0
APMPM J2352-3609[b]	23 52 27.35	-36 09 12.2	1996.6	0.31	-0.37	18.55	16.60	J=13.28	$J-K_S$=1.10	23.3

[a] Photometric distance estimate assuming that the star belongs to the disc/to the thick disc, obtained using the (M_J,$I-J$) theoretical relation from Baraffe et al. (1998) with a metallicity of 0 dex/-0.8 dex (see Reylé et al. (2002)).
[b] I drop-out star. The DENIS magnitude is in the J-band, the colour is $J-K_S$. The photometric distance has been computed using the (M_J,$J-K_S$) theoretical relation from Baraffe et al. (1998).

Table 4. Comparison stars for spectroscopic classification. The spectral types found in the literature are given, as well as the final adopted spectral types.

name	NStars	ARICNS	Simbad	other	adopted
LHS 29	–	M1	M1	sdM1.0[a]/sdM0[b]	sdM0
Gl 143.1	M0	M0	K7.0	–	M0
LHS 141	M0.5	M1.0	K7	–	M0
LHS 3833	–	M0	M0	–	M0.5
LHS 1827	M1	M1	M1/M2	–	M1
LHS 65	M3	M2	M1	–	M1.5
LHS 14	M2.5	M1.5	M1.5	–	M1.5
LHS 1208	M2	–	M2	–	M2.5
LHS 502	M4	M3	M2.5	–	M3
LHS 183	M3.5	M4	M3.5	–	M3.5
LHS 138	M4.5	M4.5	M4.5	–	M4.5
LHS 168	M5.0	M5.0	M5.0	–	M5
LHS 546	M5.5	M5.5	M5.5	–	M5.5
LHS 1326	M6	M6	M6	–	M6
DENIS J1048	–	–	M8	M9[c]	M9

[a] Gizis (1997)
[b] Nidever et al. (2002)
[c] Delfosse et al. (2001)

database of standard spectra (software program called ALLSTAR). Scholz et al. (2005) used the minimisation of the absolute differences between target and template spectra in their low-resolution classification spectroscopy.

A different approach was taken by Reid et al. (1995), who measured the strengths of the prominent TiO and CaH features of M dwarfs. They defined several indices being the ratio between the flux within a given spectral feature and the flux in a nearby pseudo-continuum region.

For the latest M dwarfs, Kirkpatrick et al. (1995) defined an index based on the VO bandstrength, whereas Kirkpatrick et al. (1999) and Martín et al. (1999) proposed spectral indices for classification down to the L type where TiO and VO bands fade due to the condensation of Ti and V to dust. The pseudo-continuum spectral ratios (namely PC3) defined by Martín et al. (1999) covers a narrower wavelength range than for the computation of indices, thus it is less sensitive to possible wavelength shifts.

Lépine et al. (2003a) pointed out that a unified scheme for the classification of M dwarfs is needed and they defined an enhanced classification based on a set of existing (Reid et al. 1995; Hawley et al. 2002) and new spectral indices that measure the most important features in the optical spectral range.

Furthermore, the classification procedure of Gizis (1997) allows us to distinguish potential subdwarfs (sdM) or extreme subdwarfs (esdM) from the M dwarfs. Accordingly, Lépine et al. (2003b) used a CaH2+CaH3 versus TiO5 diagram to discriminate between the three different object classes. This diagram was also used by Lépine et al. (2004) and Scholz et al. (2004a) when reporting the discovery of an esdM6.5 and an sdM9.5 star respectively. Figure 4 shows the locus of our candidates (filled circles) in the CaH2+CaH3 versus TiO5 diagram superimposed with the data used in

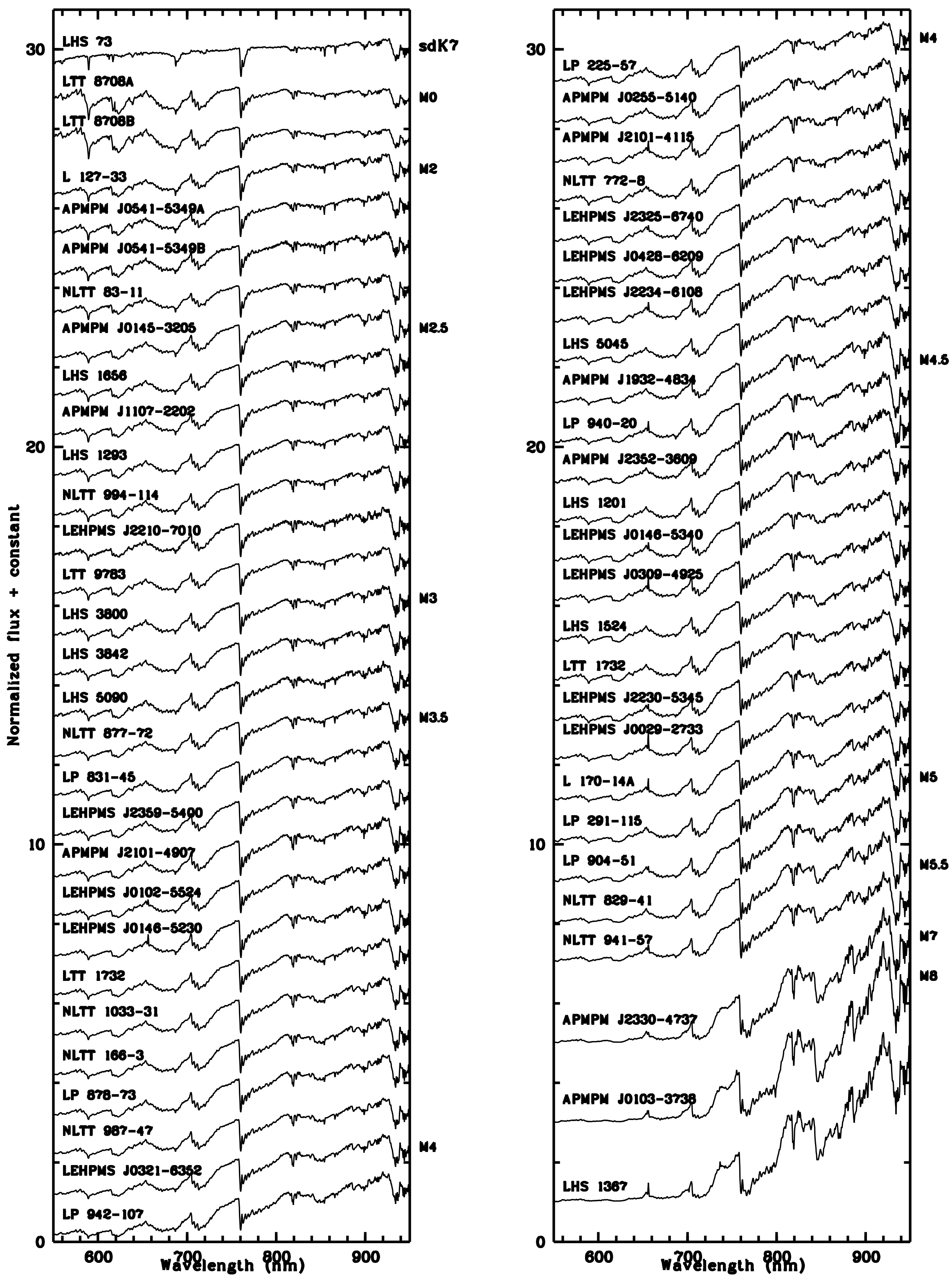

Figure 2. NTT spectra of K and M dwarfs, from spectral types K7 to M4 on the left panel, and from M4 to M8 on the right panel.

Table 3. Nearby stars candidates found in the LEHPMS observed at ESO/NTT. B_J and R are from the LEHPMS high proper motion catalogue, obtained on digitized plates. I and $I-J$ are from DENIS.

name	α_{J2000}	δ_{J2000}	ESO epoch	μ_α ("yr^{-1})	μ_δ	B_J	R	I DENIS	$(I-J)$	$d_{\rm phot}$ (pc)
LEHPMS J0029-2733	00 28 54.55	-27 33 34.3	1984.8	0.23	0.03	16.65	14.63	12.47	1.67	19.9
L 170-14A	00 29 50.33	-54 41 32.5	1988.7	-0.27	-0.22	14.51	12.89	10.99	1.64	14.6
LEHPMS J0102-5524	01 01 57.31	-55 23 47.1	1981.8	0.28	0.07	15.34	13.20	11.24	1.54	18.5
LHS 1201	01 08 46.93	-37 10 16.8	1989.7	-0.56	-0.45	17.29	14.92	12.72	1.92	17.9
LHS 1249[a]	01 24 03.54	-42 40 30.0	1983.8	0.31	-0.54	15.62	14.81	14.46	0.25	16.9
LEHPMS J0141-5544[a]	01 40 31.11	-55 43 39.4	1984.9	0.21	-0.01	15.12	15.28	14.97	-0.63	−−
LHS 1293	01 45 11.07	-32 05 09.7	1985.9	0.67	0.22	15.37	13.25	11.20	1.51	18.0
LEHPMS J0146-5230	01 45 30.37	-52 30 20.1	1984.9	0.18	0.03	15.26	13.86	12.17	1.71	17.5
LEHPMS J0146-5340	01 46 29.07	-53 39 30.9	1984.9	0.18	-0.11	15.52	13.18	10.90	1.59	12.7
LHS 1367	02 15 07.38	-30 39 57.2	1988.8	0.77	-0.34	20.23	17.34	14.03	2.46	17.4
NLTT 829-41	02 16 21.55	-22 00 52.0	1984.8	-0.12	0.22	18.14	15.55	12.74	1.96	19.6
NLTT 941-57	02 22 18.07	-36 51 52.8	1989.8	0.29	0.10	17.45	15.16	12.57	1.93	18.2
NLTT 8435[a]	02 35 21.91	-24 00 38.3	1985.8	-0.11	-0.63	16.58	15.36	14.92	0.56	14.3
LP 942-107	03 05 10.79	-34 05 23.1	1983.8	0.37	-0.05	14.41	11.97	9.72	1.55	14.8
LEHPMS J0309-4925	03 08 59.98	-49 24 53.5	1981.8	0.16	0.10	16.19	13.67	11.45	1.69	17.5
NLTT 994-114	03 09 21.59	-39 11 02.8	1981.9	0.38	-0.01	13.56	11.25	9.99	1.42	15.9
NLTT 772-8	03 09 50.86	-19 06 46.9	1986.9	0.41	-0.09	15.41	12.85	10.94	1.56	17.4
LHS 1524	03 17 17.57	-19 40 14.7	1986.9	0.53	-0.25	16.57	14.23	11.86	1.78	19.3
LEHPMS J0321-6352	03 20 51.84	-63 51 47.9	1984.7	0.04	-0.31	14.29	11.77	9.49	1.48	14.0
LTT 1732	03 38 55.65	-52 34 15.0	1981.8	0.15	0.21	15.74	13.18	11.15	1.58	14.6
LEHPMS J0428-6209	04 28 05.44	-62 09 28.6	1989.8	0.21	0.32	14.15	11.76	9.96	1.50	11.9
LEHPMS J0503-5353	05 03 24.90	-53 53 20.9	1982.0	0.48	0.10	15.61	13.14	11.02	1.64	16.6
NLTT 83-11	22 10 10.48	-70 10 06.8	1984.6	0.08	-0.27	14.03	11.78	10.53	1.46	17.9
LEHPMS J2210-7010	22 10 19.97	-70 10 04.4	1984.6	0.08	-0.26	14.88	12.66	11.17	1.67	14.2
LEHPMS J2230-5345	22 30 09.59	-53 44 44.8	1985.7	-0.03	-0.76	15.81	13.39	11.19	1.68	12.0
LEHPMS J2234-6108	22 34 04.12	-61 07 40.4	1985.5	0.26	-0.05	16.36	13.84	10.88	1.65	15.9
NLTT 1033-31	22 35 04.52	-42 17 45.3	1981.8	0.27	-0.16	14.40	11.80	10.34	1.40	18.3
NLTT 166-3	22 41 59.52	-59 15 12.2	1986.8	0.34	0.00	15.34	13.07	11.25	1.71	12.5
LEHPMS J2248-4715[a]	22 48 08.68	-47 14 45.3	1983.8	0.05	-0.29	17.77	15.84	15.26	0.50	18
NLTT 877-72	23 09 59.91	-21 11 43.1	1984.8	0.34	0.01	13.67	10.89	9.82	1.36	19.1
LEHPMS J2325-6740	23 25 24.54	-67 40 05.6	1984.8	0.24	-0.15	15.60	13.22	11.09	1.61	16.5
LP 878-73	23 40 47.99	-22 25 27.9	1986.6	-0.37	-0.25	16.36	14.10	12.07	1.77	19.2
LHS 73[b]	23 43 15.49	-24 10 47.2	1986.8	1.37	-2.20	14.03	11.72	11.17	1.09	12.3
LTT 9783	23 53 08.12	-42 32 04.5	1989.8	0.18	0.10	13.93	11.24	9.86	1.44	15.9
NLTT 987-47	23 53 40.74	-35 59 07.6	1988.8	0.30	0.16	14.77	12.46	10.68	1.43	19.1
LEHPMS J2354-3634[a]	23 54 18.80	-36 33 47.3	1988.8	0.05	-0.68	15.60	15.71	15.34	-0.50	−−
LEHPMS J2359-5400	23 58 49.37	-54 00 13.2	1989.6	-0.15	-0.16	15.64	13.05	11.57	1.56	19.6

[a] White dwarf candidates. The photometric distance has been computed with (M_J,$I-J$) theoretical relation from Bergeron et al. (1995) for 0.6M$_\odot$white dwarfs. No distances were determined for the bluest candidates as they are beyond the colour limit of the theoretical relation.

[b] Subdwarf candidate. The photometric distance has been obtained using the (M_J,$I-J$) theoretical relation from Baraffe et al. (1998) with a metallicity of -1.8 dex.

the same diagram by Lépine et al. (2003b) and newly discovered objects by Lépine et al. (2004); Scholz et al. (2004a,b); Farihi et al. (2005).

Most of our candidates lie in the M-dwarfs region, including the 4 stars for which alternative distances were computed assuming that they belong to the thick disc (see last column in Table 2). Thus these stars are more distant disc stars instead of nearby low-metallicity dwarfs.

Spectral types are obtained by visual comparison with our spectral templates of comparison stars, observed together with our target stars (Table 4). For comparison, we also derive spectral types, using the classification scheme based on the TiO and CaH bandstrengths. We also measured the pseudo-continuum spectral ratio PC3, useful for late dwarfs, in particular for M7 and M8 stars that are missing in our comparison sequence. The results are given in Table 5. The uncertainty of our spectral type determination is 0.5 subclass.

Figure 5 shows the spectral type determined from the TiO5 and PC3 indices versus our adopted spectral type obtained from the comparison with templates. As already pointed out by the different authors who defined the indices, the TiO5 index starts to deviate from our spectral sequence for spectral types later than M6, whereas the PC3 index is not reliable for stars earlier than M3. Both indices are well in agreement in the overlapping region M3-M6.

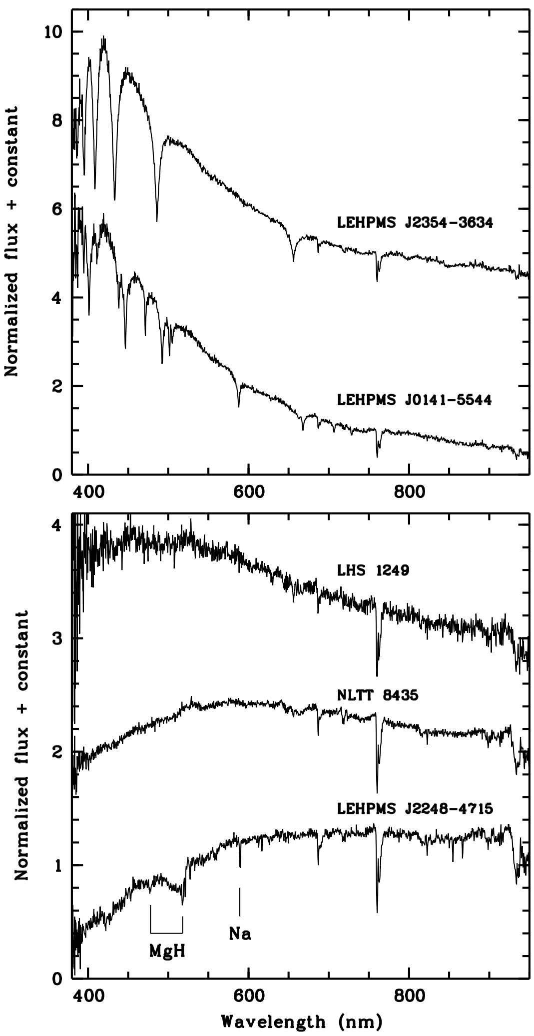

Figure 3. NTT spectra of the white dwarf candidates. Two hot white dwarfs are shown in the top panel, whereas two featureless cool white dwarfs and a K subdwarf (bottom) are shown in the lower panel.

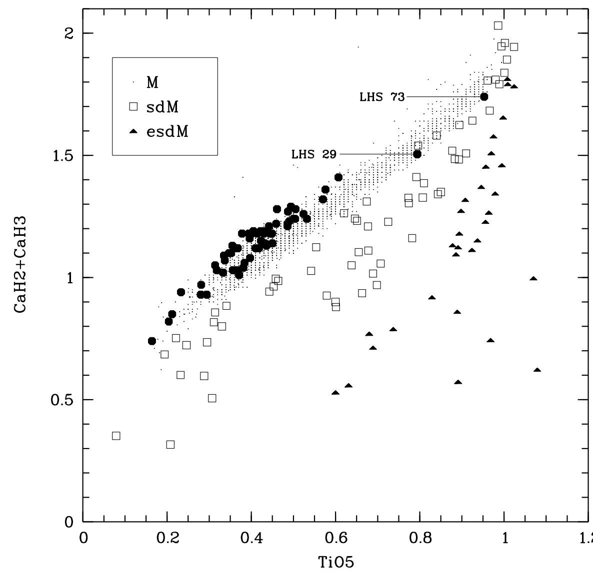

Figure 4. Relative strengths of the CaH and TiO molecular bands for spectroscopically identified M dwarfs, subdwarfs (sdM) and extreme subdwarfs (esdM) according to the classification scheme of Gizis (1997). Our nearby candidates are shown with filled circles.

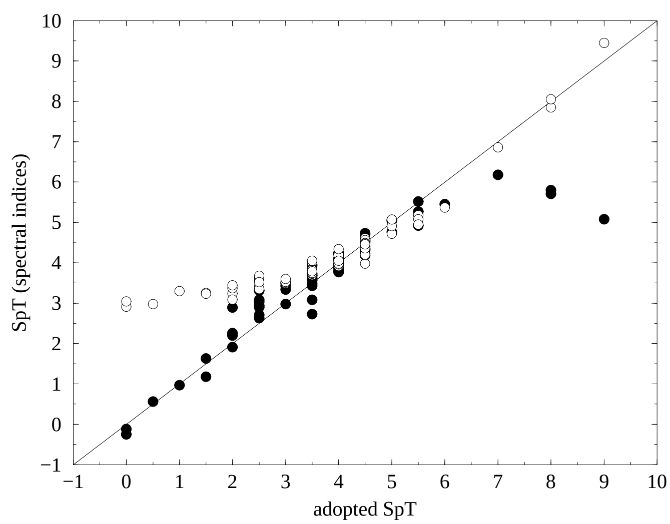

Figure 5. Spectral type obtained from the TiO5 (filled circles) and PC3 (open circles) indices versus the adopted spectral type checked against the spectra of comparison stars.

4.2 Subdwarfs

The sdM0 star LHS 29 and LHS 73 are also marked in Figure 4. The latter could also be a subdwarf given its location in the reduced proper motion versus colour diagram. Its position in the CaH2+CaH3 versus TiO5 diagram is compatible with the position of other known subdwarfs, although dwarfs, subdwarfs and extreme subdwarfs are not well separated in this part of the diagram.

For this star, LHS 73, we determined the radial velocity. We compared the position of the potassium line at 769.9 nm, the iron line at 838.8 nm, and the calcium triplet at 849.8 nm, 854.2 nm and 866.2 nm with the position of the same lines in the spectrum of the standard star LHS 1827 with known radial velocity (47.2 km s^{-1}). We obtained a radial velocity of 100.6 km s^{-1}, with an accuracy of 15 km s^{-1}. We then computed the galactocentric velocities and found (U,V,W) = (-0.4 $\pm$ 3.8,-207.0 $\pm$ 23.3,-141.4 $\pm$ 15.2) km s^{-1}, compatible with the space motion of a star belonging to an old population, thick disc or halo. Thus, following the procedure of Gizis (1997), we derived a sdK7 spectral type.

4.3 White dwarfs

The spectra of the five white dwarf candidates are shown in Figure 3. The two bluest candidates shown on the top panel are hot white dwarfs. LEHPMS J2354-3634 is an early type DA white dwarf with broad Balmer lines and LEHPMS J0141-5544 is a helium rich DB white dwarf. For such blue objects, the atmosphere models of Bergeron et al. (1995) for DA and DB white dwarfs do not give an absolute magnitude.

Table 5. Spectroscopic indices, spectral type, absolute magnitude M_J and spectroscopic distance of the red dwarf candidates observed at NTT. The additional letter "e" in the spectral type indicates a star showing H_α emission.

name	TiO5	CaH1	CaH2	CaH3	PC3	SpT	J	M_J	$d_{\rm spectro}$ (pc)	Comments
LP 291-115	0.281	0.784	0.334	0.646	1.268	M5.0	10.47	9.72	14.2±2.0	
APMPM J0103-3738	0.212	0.891	0.265	0.590	1.801	M8.0e	11.16	11.15	10.0±0.8	
APMPM J0145-3205	0.504	0.803	0.497	0.754	1.055	M2.5	9.84	7.14	34.7±2.8	
LP 940-20	0.352	0.766	0.418	0.696	1.188	M4.5e	10.89	8.84	25.7±8.4	M4.5 at d = 31.4 ± 5.3 pc[b]
LHS 5045	0.365	0.840	0.417	0.718	1.171	M4.0	9.17	8.63	12.9±4.4	
LP 225-57	0.401	0.854	0.452	0.736	1.123	M4.0	8.23	8.63	8.3±2.8	
L 127-33	0.570	0.801	0.558	0.778	1.031	M2.0	11.21	6.97	70.6±5.3	
APMPM J0255-5140	0.394	0.858	0.441	0.745	1.132	M4.0	9.89	8.63	17.9±6.1	
LP 831-45	0.444	0.808	0.464	0.727	1.102	M3.5	7.62	8.41	10.4±3.5	
LHS 5090	0.450	0.782	0.434	0.713	1.067	M3.0	11.60	7.32	71.8±6.2	
LHS 1656	0.500	0.811	0.501	0.749	1.073	M2.5	9.53	7.15	30.0±2.4	
APMPM J0541-5349A	0.576	0.794	0.575	0.798	1.048	M2.0	10.58	6.97	52.7±4.0	
APMPM J0541-5349B	0.505	0.780	0.526	0.762	1.058	M2.0	10.64	6.97	54.2±4.1	
LP 904-51	0.280	0.743	0.333	0.606	1.292	M5.0e	11.01	9.72	18.1±2.6	
APMPM J1107-2202	0.532	0.779	0.505	0.749	1.080	M2.5	9.92	7.14	36.0±2.9	
APMPM J1932-4834	0.335	0.846	0.397	0.707	1.162	M4.5	10.54	8.84	21.9±7.2	
APMPM J2101-4115	0.381	0.755	0.396	0.652	1.161	M4.0e	9.95	8.63	18.4±6.3	
APMPM J2101-4907	0.432	0.767	0.443	0.701	1.135	M3.5	9.09	8.41	13.7±4.6	
LTT 8708 A	0.487	0.766	0.537	0.749	0.886	M0.0	7.75[a]	6.33	27.2±1.8	
LTT 8708 B	0.494	0.780	0.542	0.755	0.879	M0.0	7.75[a]	6.33	27.2±1.8	
LHS 3800	0.442	0.785	0.484	0.737	1.069	M3.0	10.90	7.32	52.0±4.6	
LHS 3842	0.459	0.795	0.487	0.744	1.079	M3.0	9.75	7.32	30.6±2.6	
APMPM J2330-4737	0.164	0.769	0.233	0.510	1.596	M7.0e	11.32	10.73	13.1±1.5	M6 at d = 15.8 ± 1.9 pc[c]
APMPM J2352-3609	0.314	0.856	0.379	0.688	1.203	M4.5	12.18	8.84	46.6±15.3	
LEHPMS J0029-2733	0.368	0.820	0.421	0.703	1.162	M4.5e	10.80	8.84	24.7±8.1	
L 170-14A	0.347	0.869	0.409	0.709	1.188	M4.5e	9.35	8.84	12.7±4.1	
LEHPMS J0102-5524	0.423	0.809	0.449	0.711	1.114	M3.5e	9.70	8.41	18.2±6.2	
LHS 1201	0.318	0.780	0.370	0.663	1.215	M4.5	10.80	8.84	24.7±8.1	
LHS 1293	0.490	0.804	0.497	0.740	1.084	M2.5	9.69	7.14	32.3±2.6	
LEHPMS J0146-5230	0.436	0.803	0.441	0.692	1.097	M3.5e	10.46	8.41	25.8±8.7	
LEHPMS J0146-5340	0.371	0.761	0.380	0.637	1.204	M4.5e	9.31	8.84	12.4±4.1	
LHS 1367	0.204	0.849	0.262	0.561	1.846	M8.0e	11.57	11.15	12.1±1.0	
NLTT 829-41	0.233	0.757	0.310	0.631	1.293	M5.5	10.78	10.05	14.0±1.7	M5.5 at d = 19.3 ± 1.6 pc[b]
NLTT 941-57	0.294	0.776	0.335	0.603	1.273	M5.5e	10.64	10.05	13.1±1.6	
LP 942-107	0.405	0.839	0.450	0.741	1.128	M4.0	9.63	8.63	15.9±5.4	M4 at d = 17.9 pc[d]
LEHPMS J0309-4925	0.359	0.770	0.393	0.641	1.188	M4.5e	9.76	8.84	15.3±5.0	
NLTT 994-114	0.486	0.797	0.485	0.739	1.090	M2.5	9.00	7.14	23.5±1.9	
NLTT 772-8	0.410	0.774	0.433	0.696	1.167	M4.0	9.38	8.63	14.2±4.8	
LHS 1524	0.337	0.793	0.390	0.687	1.185	M4.5	10.08	8.84	17.7±5.8	
LEHPMS J0321-6352	0.414	0.825	0.451	0.732	1.132	M4.0	9.13	8.63	12.6±4.3	
LTT 1732	0.356	0.743	0.385	0.659	1.204	M4.5	9.57	8.84	14.0±4.6	
LEHPMS J0428-6209	0.449	0.816	0.460	0.725	1.111	M3.5	8.94	8.41	12.8±4.3	
LEHPMS J0503-5353	0.378	0.814	0.440	0.746	1.162	M4.0	9.38	8.63	14.2±4.8	
NLTT 83-11	0.607	0.856	0.609	0.818	1.011	M2.0	9.07	6.97	26.3±2.0	
LEHPMS J2210-7010	0.461	0.802	0.526	0.764	1.046	M3.5	9.50	8.41	16.6±5.6	
LEHPMS J2230-5345	0.333	0.794	0.371	0.650	1.200	M4.5	9.51	8.84	13.6±4.5	
LEHPMS J2234-6108	0.366	0.745	0.393	0.649	1.183	M4.0e	9.23	8.63	13.2±4.5	
NLTT 1033-31	0.422	0.836	0.461	0.733	1.111	M3.5	9.10	8.41	13.8±4.7	
NLTT 166-3	0.396	0.827	0.443	0.726	1.096	M3.5	9.54	8.41	16.9±5.7	
NLTT 877-72	0.486	0.796	0.486	0.742	1.109	M3.5	8.86	8.41	12.4±4.2	
LEHPMS J2325-6740	0.397	0.791	0.416	0.677	1.142	M4.0e	9.48	8.63	14.8±5.0	
LP 878-73	0.418	0.783	0.430	0.698	1.141	M3.5	10.30	8.41	23.9±8.1	
LHS 73	0.960	0.889	0.847	0.901	0.997	sdK7	10.08	8.72	18.7	
LTT 9783	0.524	0.808	0.514	0.757	1.068	M2.5	9.17	7.14	25.5±2.0	
NLTT 987-47	0.430	0.839	0.459	0.734	1.100	M3.5	9.25	8.41	14.8±5.0	
LEHPMS J2359-5400	0.431	0.836	0.466	0.735	1.105	M3.5	10.01	8.41	21.0±7.1	

[a] Total magnitude of the system [b] Reid et al. (2003b) [c] Lodieu et al. (2005) [d] Scholz et al. (2005)

To compute their distance, we used instead the relation from Oppenheimer et al. (2001)

$$M_{B_J} = 12.73 + 2.58(B_J - R)$$

We obtained d_{B_J} = 44.9 pc for LEHPMS J2354-3634. Distances were also derived by Pauli et al. (2003); Salim et al. (2004) from spectroscopic observations. They found a distance of 62.6 pc and 59 ± 14 pc respectively. From spectral fitting, Koester et al. (2001) found an effective temperature around 14500 K. For LEHPMS J0141-5544, we computed d_{B_J} = 36.3 pc.

On the bottom panel, LHS 1249 and NLTT 8435 are featureless DC white dwarfs, although they could show weak H_α absorption, in particular LHS 1249. Spectra with better signal to noise would be required to assign a DC or DA class. We derived d_{B_J} = 14.4 pc for LHS 1249 and d_{B_J} = 13.8 pc for NLTT 8435. For those objects, we also estimated the distance using the M_J versus $I - J$ theoretical relation for white dwarfs of 0.6 $M_\odot$ from Bergeron et al. (1995) and obtained 16.9 pc for LHS 1249 and 14.3 pc for NLTT 8435. Following the conventional number 50 $400/T_{\rm eff}$ to assign a spectral index, we performed black-body fits to the spectra and obtained 6200 K for LHS 1249 and 4800 K for NLTT

8435, with an accuracy of ± 100 K. The derived spectral types are DC8 and DC10, respectively. Kawka et al. (2004) obtained spectroscopy of NLTT 8435 and found it to be a DC white dwarf at 16 pc and with $T_{\rm eff} = 5300 \pm 200$ K.

The lower spectrum shows clear indications of K dwarfs (MgH, Na features). LEHPMS J2248-4715 is not a nearby white dwarf but a distant K subdwarf. Following the spectral classification scheme of Gizis (1997), we measured the Ti05, CaH1, CaH2, and CaH3 indices and estimated a spectral type sdK5.

5 SPECTROSCOPIC DISTANCES

5.1 M dwarfs

Spectral type versus absolute magnitudes relations can be used to derive the distances of our red dwarf targets. Reid et al. (1995); Henry et al. (1994, 2002) computed relations between spectral type and absolute magnitude in the V band, Lépine et al. (2003a) in the R, B, and K_s bands.

Several calibrations have also been computed in the J-band:

Dahn et al. (2002) determined trigonometric parallaxes for 28 late-type dwarfs and derived a M_J(spectral type) relation valid for types later than M6.5.

Hawley et al. (2002) used a well observed sample of nearby dwarfs with measured trigonometric parallaxes, 2MASS J magnitude and spectral type to calibrate a spectroscopic parallax relation M_J(spectral type). They adopted a fit with several line segments in the spectral type range from K7 to T8.

Cruz & Reid (2002) used a sample of 68 late-type dwarfs with well determined trigonometric parallaxes surveyed by the Palomar/Michigan State University (PMSU) survey to derive a M_J(TiO5) relation. Cruz et al. (2003) suplemented these data to fit a fourth-order polynomial M_J(spectral type) relation, valid for types M6 to L8.

Scholz et al. (2005) provided M_J for spectral types over the whole range from K0 to L8.

Crifo et al. (2005) identified in the literature 27 stars with good trigonometric parallaxes and photometry and with known PC3 indices to derive a calibration of absolute magnitudes in the near infrared as a function of the PC3 index.

Since the more accurate available photometry of our candidates is in the near infrared bands, we prefer to use spectral type versus near infrared absolute magnitudes relations. The available M_J against spectral type calibration relations are shown in Figure 6, in the spectral type range where they are valid. We note that the absolute magnitudes M_J given by most of calibration relations do not differ by more than the differences due to the 0.5 subclass uncertainty in the spectral type.

For types earlier than M3.5, we computed the mean of the M_J obtained using Hawley et al. (2002) and Cruz & Reid (2002) relations. For the stars falling in the region M3.5 to M4.5, where there is a clear discontinuity in the calibrating relations (see Reid & Cruz 2002, for a discussion on this jump), we averaged the absolute magnitudes obtained from the upper (Cruz & Reid 2002) and lower relations (Cruz & Reid 2002; Crifo et al. 2005), as well as the fixed value $M_J = 8.34$ (Hawley et al. 2002). For types M5 to M6, we used the relations by Cruz & Reid (2002) and Crifo et al. (2005). For later types, the relations are nearly equal. For practical reasons, we only used the relation by Cruz et al. (2003) which is directly given as a function of spectral type. The filled circles in Figure 6 show the result of this combination of existing calibrating relations. The values provided by Scholz et al. (2005) are shown for comparison (pluses).

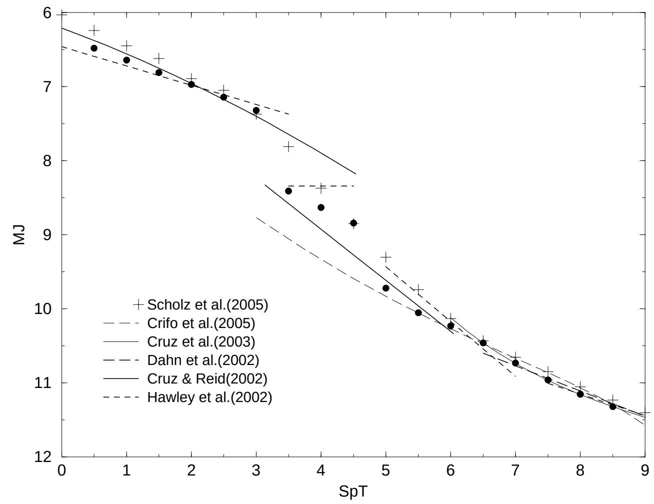

Figure 6. M_J vs spectral type calibration relations from Crifo et al. (2005) (long dashed line), Cruz et al. (2003) (thin line), Hawley et al. (2002) (thick dashed line), Cruz & Reid (2002) (thick line), and Dahn et al. (2002) (long dashed thick line). For the Crifo et al. (2005) and Cruz & Reid (2002) relations, the PC3 and TiO5 indices had first to be transformed to spectral types, respectively. The calibration we adopted is a combination of these relations, and is shown by the filled circles. For comparison, the pluses show the values given by Scholz et al. (2005). Spectral types are from M0 to M9.

The resulting values of M_J and spectroscopic distances of our candidates are given in Table 5. The uncertainties are also given, taking into account the 0.5 subclass uncertainty on the spectral type. They are less than 15%. For the spectral types M3.5 to M4.5, the uncertainties are computed given the upper and lower calibrations. The are larger, ∼ 34%. For the brightest stars with $J < 9$, we used 2MASS J magnitudes instead of DENIS due to saturation problems that may occur in the DENIS bands.

Other determinations of spectral types and spectroscopic distances are given in Table 5. They are in agreement with our values.

5.2 Subdwarf

We computed the distance of the subdwarf LHS 73 assuming an absolute magnitude $M_J = 8.72$, following Reid & Gizis (2005). The resulting distance is 18.7 pc. LHS 73 has a common proper motion companion, LHS 72, with a separation of 94″. LHS 72 has been spectroscopically classified as a subdwarf by Rodgers & Eggen (1974). A quite uncertain trigonometric parallax, 37.6 ± 8.9 mas (21.5 pc $< d <$ 34.8 pc) can

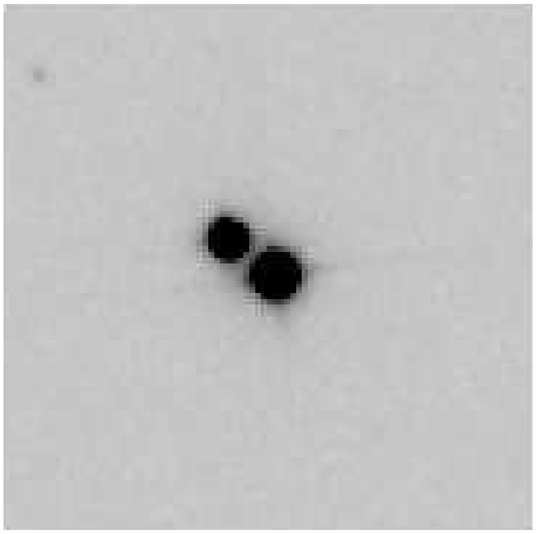

Figure 7. Part of the R-band NTT image of the binary APMPM J0541-5349. The size of the image is 30″× 30″. North is up, East is to the left.

be found for this star in the Yale Trigonometric Parallaxes (van Altena et al. 1995).

Most K/M subdwarfs with trigonometric parallaxes are listed in Gizis (1997). Only a handful of these (LHS 20, LHS 29, LHS 35, LHS 44, LHS 55, LHS 103, LHS 3409) are within 20 pc. Another pair of subdwarfs LHS 52/LHS 53, is slightly more distant ($d = 29.8 \pm 1.5$ pc). To our knowledge, LHS 72/LHS 73 is the closest pair of subdwarfs.

5.3 Binaries

Besides LHS 73 which belongs to a common proper motion pair (§ 5.2), two objects in our sample are binaries.

LTT 8708A/B is an already known system. We used the acquisition image, obtained in the ESO R-band, to derive a separation of 8.1 pixels. With a scale of 0.33″/pixel, this corresponds to an angular separation of 2.7″. The spectra of the two components show that they are both M0 stars, with absolute magnitudes $M_J = 6.33$. With an observed total magnitude $J = 7.75$, we derived a distance of 27.2 ± 1.8 pc. This result is in agreement with the trigonometric parallax derived by Hipparcos, although the uncertainty was very large (74.42 mas ± 41.23 or a distance between 8.6 pc and 30.1 pc). Hawley et al. (1997) found a smaller distance, $d = 17.5$ pc, and a spectral type of M2.5.

APMPM J0541-5349 is clearly seen as a binary on the acquisition image (Figure 7). The separation between the components is 10.1 pixels, corresponding to 3.33″. The examination of earlier images such as 2MASS or DSS2 show that they are a common proper motion pair. Two objects are given in the 2MASS point source catalogue, with magnitudes $J = 10.58$ and 10.64. Both components have a M2 spectral type, and an absolute magnitude $M_J = 6.97$. Thus the system is at a distance of 53.4 ± 4.1 pc.

6 CHROMOSPHERIC ACTIVITY

H_α is a chromospheric activity indicator for M dwarfs. Stars showing a H_α emission line are indicated by the additional letter "e" in the spectral type column of Table 5. Although the size of our sample is too small to have a strong statistical sense, we find a correlation between the activity and the spectral type. The number of active stars is greater among late-type stars than early-type stars and is increasing across the spectral type sequence. None of the stars with spectral type earlier than M3 (over 14 objects) shows an H_α emission line, whereas all of our three stars later than M8 show evidence of activity. 24% of the M3.5-M4 stars (over 21 objects), and 47% of the M4.5 to M6 stars (over 16 objects) show activity. This is consistent with the fraction of objects with H_α in emission versus spectral type reported by Gizis et al. (2000) from a larger sample of M dwarfs.

7 CONCLUSION

We obtained spectral types and spectroscopic distances for 59 high proper motion stars. These stars are nearby candidates, as seen from their photometric distances. 42 stars have indeed spectroscopic distances below the 25 pc limit of the Catalogue of Nearby Stars. These new neighbours are few in regards to the large number of missing stellar systems within 25 pc ($\sim$ 2000) according to Henry et al. (2002). However, this study, joined to similar ones, allows to increase, step by step, the completeness of the solar neighbourhood sample and to cross-check the new nearby candidates in different samples (see e.g. Table 1). Nevertheless, it is clear that further efforts are needed in order to reach a much higher completeness level.

The neighbours recovered from our study are mainly M dwarfs. Three are white dwarfs, cooler than 6200 K. One star, APMPM J0541-5349, appeared to be a binary consisting of two M2 stars with an angular separation of 3.33″, at a distance of 53.4 ± 4.1 pc from the Sun. We computed the radial velocity of the subdwarf candidate LHS 73 and found a space motion compatible with that of an object belonging to an old population. With our determined distance of 18.7 pc, LHS 73 is among the few subdwarfs within 20 pc. Furthermore, LHS 73 has a companion, LHS 72. LHS 72/LHS 73 is probably the closest known pair of subdwarfs. Two stars lie within 10 pc: APMPM J0103-3738 is a M8 star at distance d = 10.0 ± 0.8 pc, and LP 225-57 a M4 star at d = 8.3 ± 2.8 pc.

The new sources that we identified are worthy of more detailed observations, including high-resolution imaging to search for low-mass companions, and trigonometric parallax measurements. We plan more follow-up for the nearest objects and hope to place the most promising targets on new or existing parallax programs such as that of the Cerro Tololo Inter-American Observatory Parallax Investigation (Jao et al. 2005, CTIOPI).

ACKNOWLEDGMENTS

Céline Reylé acknowledges help during the observations by Olivier Hainaut and the NTT team at the European Southern Observatory. This research has made use of the VizieR database, operated at CDS, Strasbourg, France.

REFERENCES

Baraffe, I., Chabrier, G., Allard, F., & Hauschildt, P. H. 1998, A&A, 337, 403
Bergeron, P., Wesemael, F., & Beauchamp, A. 1995, PASP, 107, 1047
Crifo, F., Phan-Bao, N., Delfosse, X., Forveille, T., Guibert, J., Martín, E. L., & Reylé, C. 2005, A&A, 441, 653
Cruz, K. L., & Reid, I. N. 2002, AJ, 123, 2828
Cruz, K. L., Reid, I. N., Liebert, J., Kirkpatrick, J. D., & Lowrance, P. J. 2003, AJ, 126, 2421
Cutri, R. M., Skrutskie, M. F., Van Dyk, S., et al. 2003, The 2MASS All-Sky Catalog of Point Sources, University of Massachusetts and IPAC/California Institute of Technology
Dahn, C. C., Harris, H. C., Vrba, F. J. et al. 2002, AJ, 124, 1170
Delfosse, X., Forveille, T., Martín, E. L. et al. 2001, A&A, 366, L13
Epchtein, N., de Batz, B., Capoani, L. et al. 1997, The Messenger, 87, 27
Farihi, J., Wood, P. R., Stalder, B. 2005, ApJ, 627, L41
Gizis, J. E. 1997, AJ, 113, 806
Gizis, J. E., Monet, D. G., Reid, I. N., Kirkpatrick, J. D., Liebert, J., & Williams, R. J. 2000, AJ, 120, 1085
Gliese, W. & Jahreiß, H. 1991, On: The Astronomical Data Center CD-ROM: Selected Astronomical Catalogs, Vol. I; L.E. Brotzmann, S.E. Gesser (eds.), NASA/Astronomical Data Center, Goddard Space Flight Center, Greenbelt, MD
Hambly, N. C., Henry, T. J., Subasavage, J. P., Brown, M. A., & Jao, W.-C. 2004, AJ, 128, 437
Hawley, S. L., Gizis, J. E., & Reid, N. I. 1997, AJ, 113, 1458
Hawley, S. L., Covey, K. R., Knapp, G. R. et al. 2002, AJ, 123, 3409
Henry, T. J., Kirkpatrick, J. D., & Simons, D. A. 1994, AJ, 108, 1437
Henry, T. J., Ianna, P. A., Kirkpatrick, J. D., & Jahreiß H. 1997, AJ, 114, 388
Henry, T. J., Walkowicz, L. M., Barto, T. C., Golimowski, D. A. 2002, AJ, 123, 2002
Jao, W.-C., Henry, T. J., Subasavage, J. P., Brown, M. A., Ianna, P. A., Bartlett, J. L., Costa, E., & Méndez, R. A. 2005, AJ, 129, 1954
Kawka, A., Vennes, S., & Thorstensen, J. R. 2004, AJ, 127, 1702
Kirkpatrick, J. D., Henry, T. J., & McCarthy, D. W. 1991, ApJS, 77, 417
Kirkpatrick, J. D., Henry, T. J., & Simons, D. A. 1995, AJ, 109, 797
Kirkpatrick, J. D., Reid, I. N., Liebert, J. et al. 1999, ApJ, 519, 802
Koester, D., Napiwotzki, R., Christlieb, N. et al. 2001, A&A, 378, 556
Lépine, S., Rich, R. M., & Shara, M. M. 2003a, AJ, 125, 1598
Lépine, S., Shara, M. M., & Rich, R. M. 2003b, ApJ, 585, L69
Lépine, S., Shara, M. M., & Rich, R. M. 2004, ApJ, 602, L125
Lodieu, N., Scholz, R.-D., McCaughrean, M. J. et al. 2005, A&A, 440, 1061
Martín, E. L., Delfosse, X., Basri, G., Goldman, B., Forveille, T., & Zapatero Osorio, M. R. 1999, AJ, 118, 2466
Nidever, D. L., Marcy, G. W., Butler, R. P., Fischer, D. A., & Vogt, S. S. 2002, ApJS, 141, 503
Oppenheimer, B. R., Hambly, N. C., Digby, A. P. et al. 2001, Sciences, 292, 698
Pauli, E.-M., Napiwotzki, R., Altmann, M., Heber, U., Odenkirchen, M., & Kerber, F. 2003, A&A, 400, 877
Phan-Bao, N., Guibert, J., Crifo, F. et al. 2001, A&A, 380, 590
Phan-Bao, N., Crifo, F., Delfosse, X. et al. 2003, A&A, 401, 959
Phan-Bao & Bessel, 2006, A&A, 446, 515
Pokorny, R. S., Jones, H. R. A., & Hambly, N. C. 2003, A&A, 397, 575
Reid, I. N., Hawley, S. L., & Gizis, J. E. 1995, AJ, 110, 1838
Reid, I. N., & Cruz, K. L. 2002, AJ, 123, 2806
Reid, I. N., Kilkenny, D., & Cruz, K. L. 2002, AJ, 123, 2822
Reid, I. N., Cruz, K. L., Laurie, S. P. et al. 2003a, AJ, 125, 354
Reid, I. N., Cruz, K. L., Allen, P. et al. 2003b, AJ, 126, 3007
Reid, I. N., Cruz, K. L., Allen, P. et al. 2004, AJ, 128, 463
Reid, I. N., & Gizis, J. E. 2005, PASP, 111, 676
Reylé, C., Robin, A. C., Scholz, R.-D., & Irwin, M. 2002, A&A, 390, 491
Reylé, C., & Robin, A. C. 2004, A&A, 421, 643
Rodgers, A. W., & Eggen, O. J. 1974, PASP, 86, 742
Salim, S., Rich, R. M., Hansen, B. M., Koopmans, L. V. E., Oppenheimer, B. R., & Blandford, R. D. 2004, ApJ, 601, 1075
Scholz, R.-D., Irwin, M., Ibata, R., Jahreiß, H., & Malkov, O. Y. 2000, A&A, 353, 958
Scholz, R.-D., McCaughrean, M. J., Lodieu, N., & Kuhlbrodt, B. 2003, A&A, 398, L29
Scholz, R.-D., Lehmann, I., Matute, I., & Zinnecker, H. 2004a, A&A, 425, 519
Scholz, R.-D., Lodieu, N., & McCaughrean, M. J. 2004b, A&A, 428, L25
Scholz, R.-D., Meusinger H., & Jahreiß, H. 2005, A&A, 442, 211
Teegarden, B. J., Pravdo, S. H., Hicks, M. et al. 2003, ApJ, 589, L51
van Altena, W. F., Lee, J. T., & Hoffleit, E. D. 1995, New Haven, CT: Yale University Observatory, —c1995, 4th ed., completely revised and enlarged,